Supplemental Information

Unregulated Active and Close Textile Mills Represent a Significant Vector of PFAS Contamination into Coastal Rivers

Matthew Dunn[1], Nicholas Noons[2], Simon Vojta[1], Jitka Becanova[1], Heidi Pickard[3], Elsie Sunderland[3], Rainer Lohmann[1]

1.Graduate School of Oceanography, University of Rhode Island
2.Rhode Island Department of Environmental Management
3. Harvard University John A. Paulson School of Engineering and Applied Sciences

Corresponding Author: rlohmann@uri.edu, Tel (1) 401-874-6612

The SI contains 14 pages, 5 figures, with 9 tables in a separate excel spreadsheet.

Table of Contents

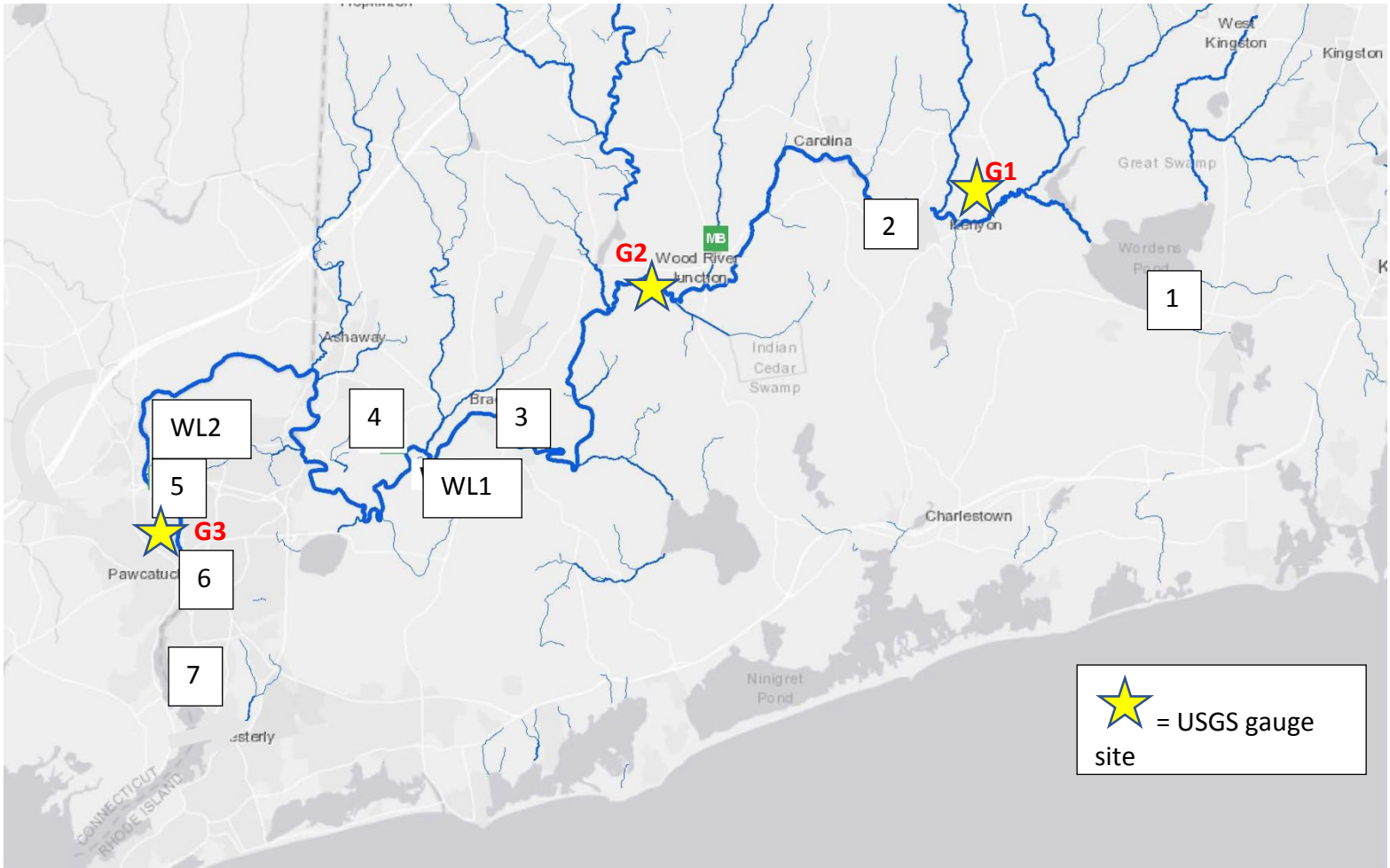

Figure S1. Map of the Pawcatuck River with corresponding site numbers and location of USGS gauge sites.

Determination of Sampling Rates. Four different groups of sampling rate data were used to calculated time weighted average (TWA) concentrations from the mass of PFAS measured in passive samplers for 9 compounds.[1–5] These included two numerical model predictions for sampling rate and two field measured sampling rates.[1–6] These calculated values were then compared to the measured grab samples from the deployment of recovery of the corresponding passive samplers and the sampling rate data that provided the best agreement between predicted and measured TWA concentrations was used throughout the rest of the study (Fig 1, Fig S1)

Explanation of Two Modeling Approaches for Sampling Rate. Two sampling rate modeling approaches explored in previous publications were applied to the passive samplers in this study to calculate time weighted average concentrations from the mass of PFAS measured in each tube.[1-5] This calculation of time weighted average concentration (*TWA* C_w) is described in equation 1,

$$TWA\ C_w = \frac{N_s}{(R_s * 86.4)\ * t} \text{ (eqn 1),}$$

where N_s is the mass (ng) of a given PFAS compound extracted from the tube passive sampler,

R_s is the sampling rate (cm s^{-1}) multiplied by a unit conversion factor of 86.4 (mL day^{-1}), and *t* is the number of days deployed in the environment.

To use equation 1, a sampling rate value must be predicted or known for each PFAS compound at a given temperature. Equation 2 describes a modeling approach for sampling rate

with no impacts of partitioning to the sorbent or membrane phases of the passive sampler included in the equation.[1,2,5] Diffusion through a porous, tortuous path is the primary pathway for PFAS into the passive sampler by this explanation.

$$\frac{1}{k_0} = \frac{1}{k_w} + \frac{d_m * {\tau_m}^2}{(D_w * \emptyset_m)} + \frac{d_{sbl} * {\tau_s}^2}{(D_w * \emptyset_s)} \text{ (eqn 2),}$$

where d_m is the thickness (cm) of the high-density polyethylene membrane,

d_{sbl} is the assumed thickness (cm) of the sorbent boundary layer at steady state conditions, which is 0.33 * the half thickness of the sorbent,

k_w is the mass transfer (cm s^{-1}) through the water boundary layer as described by Glanzmann et al. 2022,

τ_m is the tortuosity of the flow path through the membrane pore space, which is always assumed to be 1, and

τ_s is the tortuoisity of the flow path through the sorbent bed, which is assumed to be 1.3 from other sorbent modeling literature,

D_w is the aqueous diffusivity (cm^2/s) of a given PFAS compound in water at a given temperature,

And $\emptyset_m$ *and* $\emptyset_s$ are the given porosities (%) of the membrane and sorbent layers.

$$\frac{1}{k_0} = \frac{1}{k_w} + \frac{d_m}{K_{mw} * (D_w * \emptyset_m)} + \frac{d_{sbl}}{K_{sw} * (D_w * \emptyset_s)} \text{ (eqn 3)}$$

where additional terms K_{mw} and K_{sw} are the respective partitioning coefficients (g water g phase^{-1}) for PFAS to the passive sampler membrane and sorbent layers.

Equation 3 describes a model for sampling rate that includes partitioning to both the sorbent and membrane phases, as well as diffusion through porous pathways. This equation was suggested in previous works as a more accurate modeling sampling rate in tube passive samplers across short, 14-day deployments due to the importance of partitioning to the membrane of the passive sampler for longer chain or high molecular mass PFAS compounds.[1–3]

For this study, all deployments were greater than 28 days, well past the recommended deployment that equation 3 has been validated for. Thus, we can expect sampling rates to decrease as uptake slows across time as displayed by previous research.[1] This suggests that equation 2, while flawed in its disregard of partitioning, is closer in magnitude to the lower sampling rates these samplers likely exhibited across long term deployments in a matrix-rich environment.

The comparison of these predicted TWA concentrations, as well as those calculated using field observed sampling rates from two previous publications, to measured concentrations from discrete grab samples is shown in Figure S1. These grab samples were taken at the start or end of passive sampler deployments in the Pawcatuck River at all sites throughout the yearlong study. Field measured passive sampling rates from two prior publications were adjusted for temperature using the average change in sampling rate with temperature derived from the models in eqn 2 and 3 and included in this comparison as well.

When time weighted average concentrations, calculated from modeled or field measured sampling rates, were plotted against measured grab samples, the approach with the

highest slope (0.22) and closes to 1 was the sampling rates from Gardiner et al. 2022. These results were in line with previous conclusions from Dunn et al. 2022 that sampling rate increases with chain length and that sampling rates should be low for field deployments greater than 16 days. The time weighted average concentrations reported in the main text will be calculated using the mean sampling rates reported by Gardiner et al. 2022, with an adjustment of +/- 42% for every 10 ℃ change in water temperature as reported by Dunn et al. 2022.[1,6]

Environmental Details. Additional water temperatures were measured by the USGS bi-monthly at the other gauge sites and ranged from 9.9-15 ℃ in spring months, 19-25 ℃ in summer, 1.2-4.6 ℃ in winter, 13-17 ℃ in the fall. For this reason, modeled sampling rates for 5 ℃ were used for winter month calculations of time weighted average concentration, 15 ℃ model results were used for spring and fall, and 25℃ model results were used for the summer. All flow speeds were assumed to be >0.5 cm s^{-1}, based on handheld flow meter measurements all always exceeding 10 cm s-1 during field visits and visibly high flows in the river, as discussed in previous work.[1] Monthly sum precipitation data was pulled from Weather Spark, which collects and reports the atmospheric data recorded by the nearest airport in Rhode Island, T.F. Green Airport (Table S3).[7]

Quality Assurance and Quality Control Details. Blank correction for target analysis of passive and active samples was done by subtracting the average blank concentration from the sample concentration if the blank concentration was 10-30% of the sample concentration. Total blanks run was equivalent to roughly 10% of all samples analyzed. Instrumental detection limits (IDLs) were calculated using the signal to noise ratio (S/N) and calibration curve to quantify the concentration at a S/N of 10. One half of the IDL was used to

replace non detects in blank samples for calculation of the method detection limit (MDL) which is discussed in the main text. Recoveries were calculated as the peak area of the surrogate measured in the concentrated sample divided by the peak area of the surrogate in the calibration curve, with both spiked to a goal concentration of 4 ng mL^{-1}. For active grab sample quality control, targeted analysis solid phase extraction efficiency was evaluated using matrix spikes. 50 mL of tap water was spiked with 4 ng of high purity PFAS standards, including 11 of the 12 compounds discussed in this study. A matrix blank showed no contamination or detection of PFAS compounds in the tap water volume used for these experiments. The results of this matrix spike for the 11 compounds reported in this study plus 2 additional compounds can be found in Table S4 and show good recovery (84-110%).

For EOF analysis, ceramic boat blanks were analyzed twice between each set of duplicate sample injections to determine background fluorine (F) levels between sample injections. Samples were blank-corrected using the peak areas of the boat blanks run before and after each set of injections and sample concentrations were determined from the average peak areas of duplicate injections (relative standard deviation (RSD) between duplicates ≤44%, average of 10%) using a twelve point calibration curve (R2>0.998) of PFOA in methanol from 50 to 10,000 µg F/L. Quality control points were included after every 12 samples and had a variance of ≤15%. Extraction blanks were used to determine the limit of detection (LOD), which was calculated as the average plus three times the standard deviation of duplicate injections of extraction blanks. The extraction LOD was determined to be 98 ng F/mL for the passive samplers, and individual sample MDLs were calculated based on the extraction LOD multiplied by each sample's dilution factor based on sample and extract volumes. Sample MDLs ranged

from 44.7 - 65.9 ng F/sampler for the passive samplers. Sample concentrations above the MDL were adjusted for the dilution factor and corrected by subtracting the average extraction blank concentration. Complete removal was reported of a 500 ug L^{-1} spike fluoride spike on a dry passive sampler prior to extraction using a 6 mL rinse of 0.01 v/v ammonium hydroxide in mili-Q water. Samples were measured for EOF using a combustion ion chromatograph (CIC) with a combustion unit from Analytik Jena (Jena, Germany) and a 920 Absorber Module and 930 Compact IC Flex ion chromatograph from Metrohm (Herisau, Switzerland). Sample extracts (100 µL) were injected into the combustion unit at 1050 °C, and the anions were separated with an ion exchange column (Metrosep A Supp 5-150/4) operated at 30 °C, with sodium carbonate−bicarbonate buffer as eluent and isocratic elution. The fluorine (F-) concentration was measured via ion conductivity.

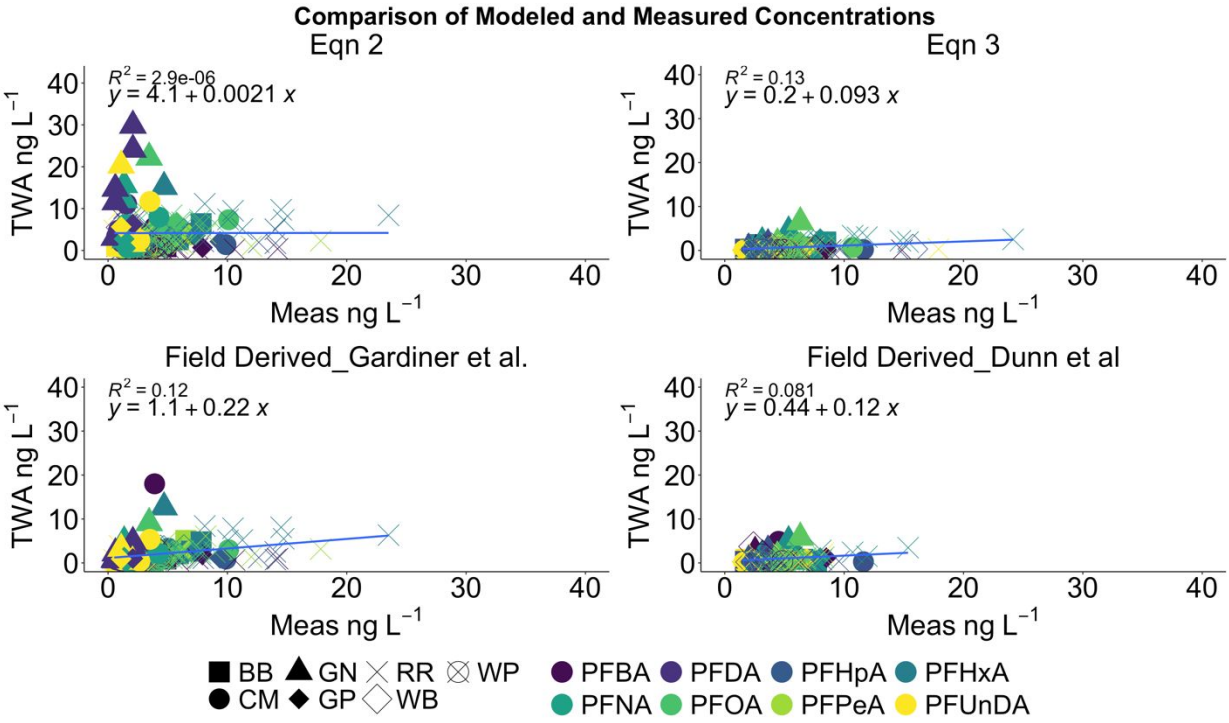

Figure S2. Predicted time weighted average concentrations from four modeling approaches compared to measured discrete grab samples. Discrete grab samples from 7 riverine and estuarine sites were extracted and compared to two modeling approaches from previous literature (Dunn et al, Vrana et al, Glanzmann et al, Booij et al). Two field measured sampling rate data sets from previous literature were also examined (Gardiner et al, Dunn et al). The data that provided the slope closest to 1 (Gardiner et al.) was used for determining final time weighted average concentrations from passive sampler results in this study.

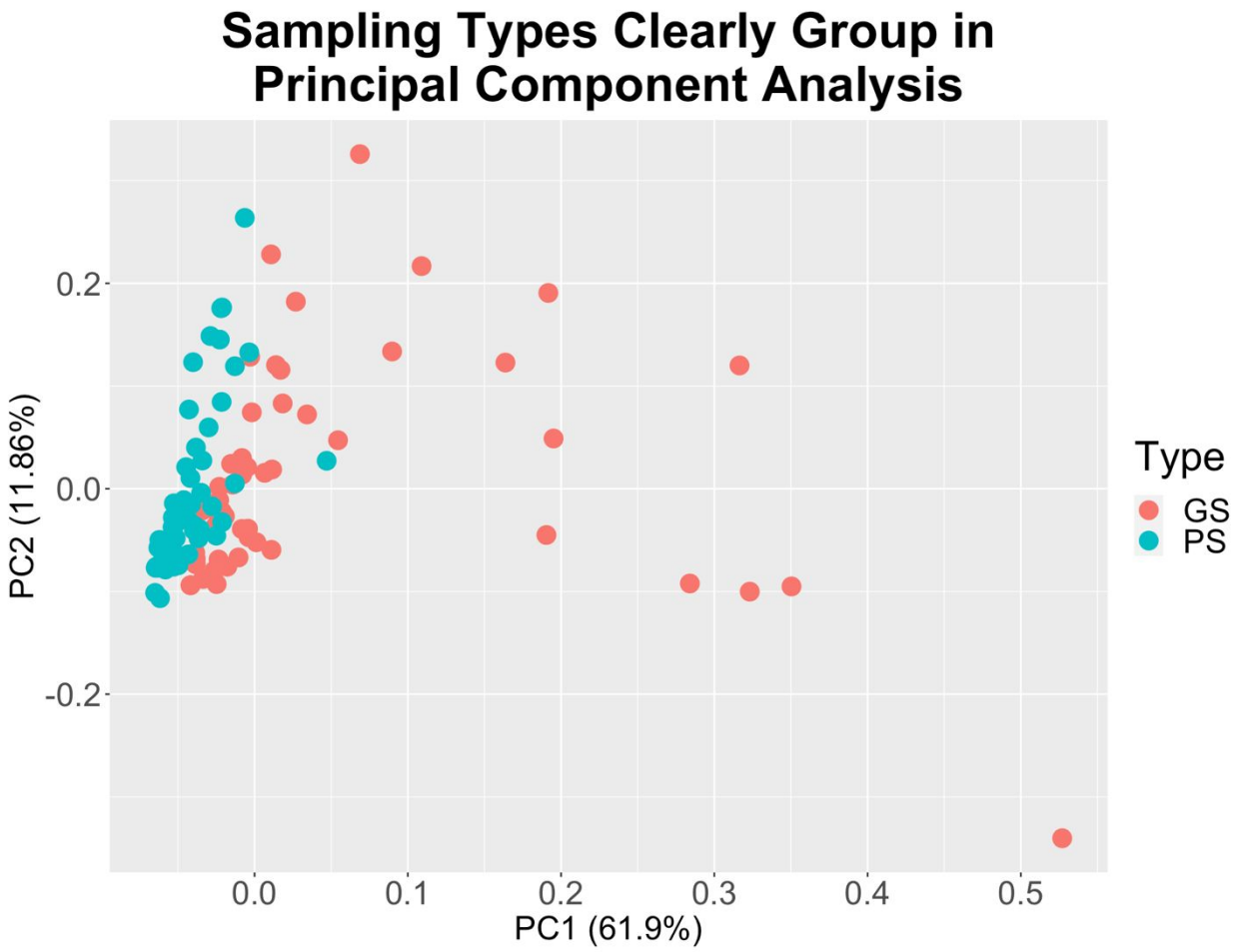

Figure S3. Principal Component Analysis Shows Grouping by Sample Type. Passive samplers (PS) are well separated from active grab samples (GS), supporting the assertion that passive samplers' produce a more smoothed, time weighted average concentration compared to the larger spread in the grab sample data.

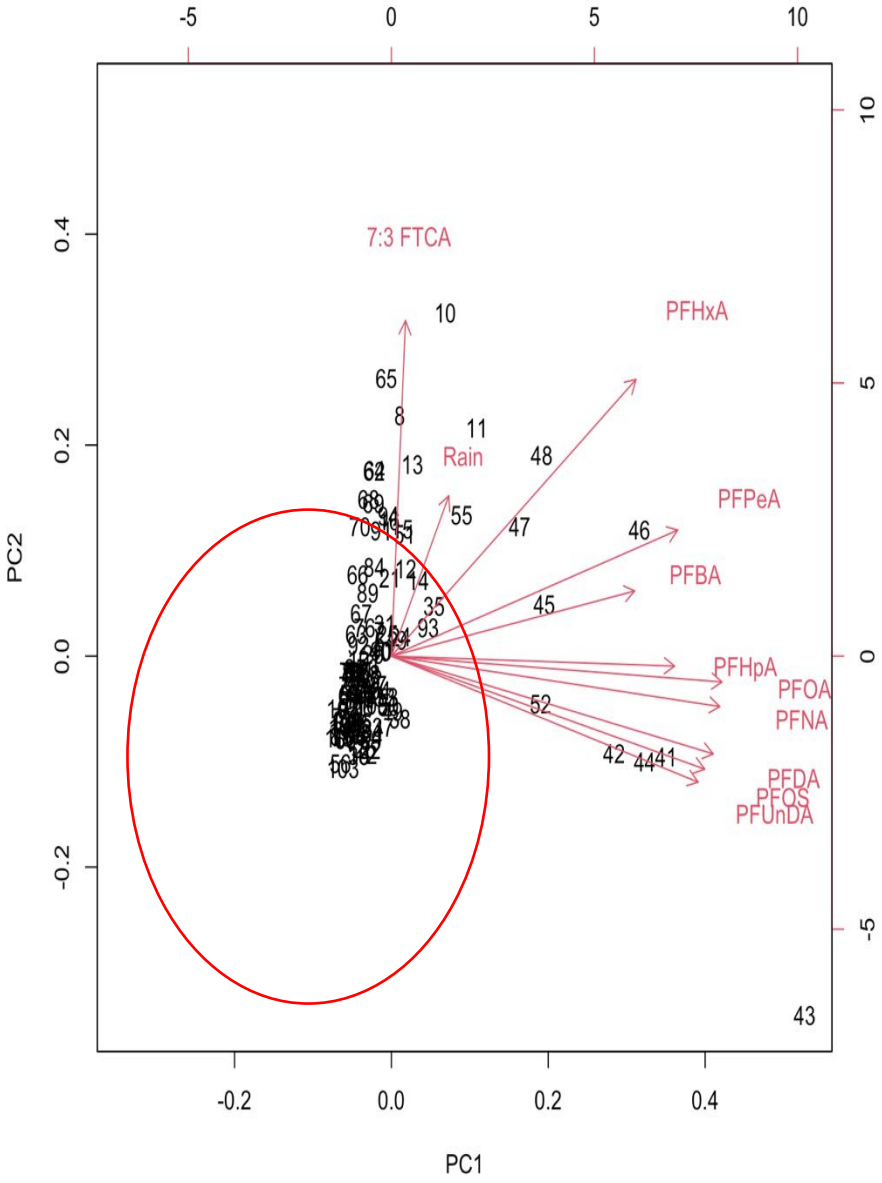

Figure S4. Principal Component Bi Plot Showing Directionality. This analysis supports the strong directionality of 7:3 FTCA as a tracer for the active mill fingerprint upstream. Furthermore, it highlights the use of PFNA, PFDA, PFUnDA (long chain PFCAs) and PFOS as indicators of historical waste lagoon impact. Rain does not appear to be a significant driver of directionality in this data set.

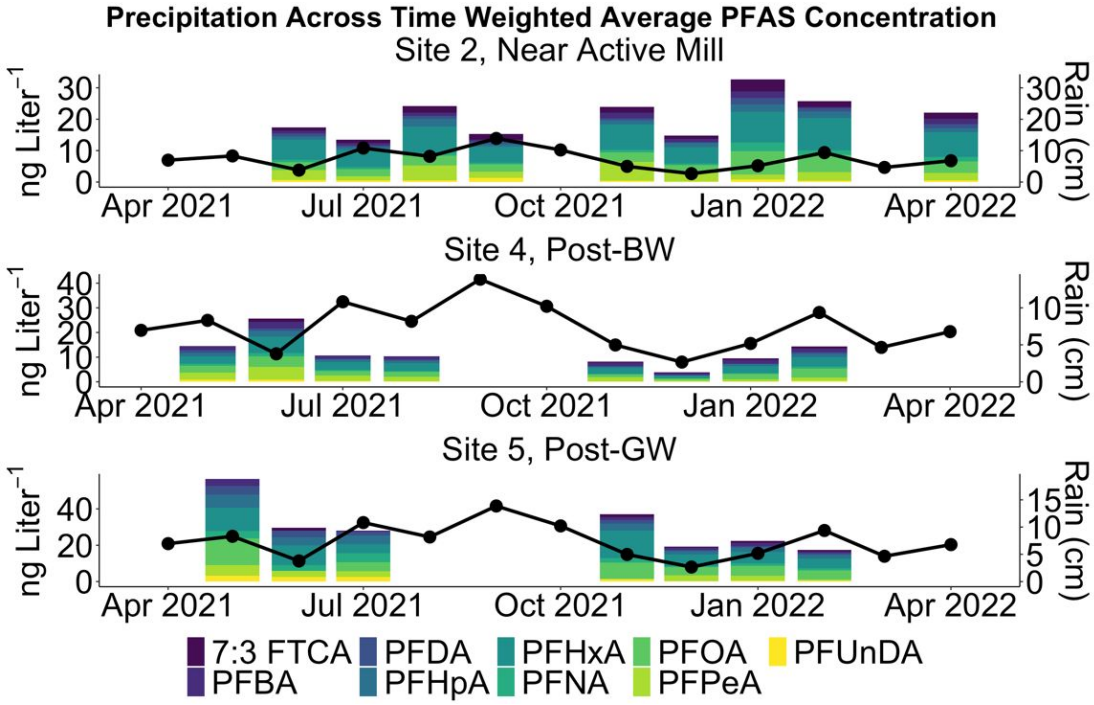

Figure S5. Monthly rainfall overlayed across time weighted average concentrations of PFAS at three sites shows marginal visible evidence of correlation.

(1) Dunn, M.; Becanova, J.; Snook, J.; Ruyle, B.; Lohmann, R. Calibration of Perfluorinated Alkyl Acid Uptake Rates by a Tube Passive Sampler in Water. *ACS EST Water* **2023**, acsestwater.2c00384. https://doi.org/10.1021/acsestwater.2c00384.
(2) Glanzmann, V.; Booij, K.; Reymond, N.; Weyermann, C.; Estoppey, N. Determining the Mass Transfer Coefficient of the Water Boundary Layer at the Surface of Aquatic Integrative Passive Samplers. *Environ. Sci. Technol.* **2021**, No. i. https://doi.org/10.1021/acs.est.1c08088.
(3) Vrana, B.; Allan, I. J.; Greenwood, R.; Mills, G. A.; Dominiak, E.; Svensson, K.; Knutsson, J.; Morrison, G. Passive Sampling Techniques for Monitoring Pollutants in Water. *TrAC - Trends Anal. Chem.* **2005**, *24* (10), 845–868. https://doi.org/10.1016/j.trac.2005.06.006.
(4) Endo, S.; Matsuura, Y. Mechanistic Model Describing the Uptake of Chemicals by Aquatic Integrative Samplers: Comparison to Data and Implications for Improved Sampler Con Fi Gurations¨. **2019**, No. 1. https://doi.org/10.1021/acs.est.8b06225.
(5) Booij, K. Passive Sampler Exchange Kinetics in Large and Small Water Volumes under Mixed Rate Control by Sorbent and Water Boundary Layer. *Environ. Toxicol. Chem.* **2021**, etc.4989. https://doi.org/10.1002/etc.4989.
(6) Gardiner, C.; Robuck, A.; Becanova, J.; Cantwell, M.; Kaserzon, S.; Katz, D.; Mueller, J.; Lohmann, R. Field Validation of a Novel Passive Sampler for Dissolved PFAS in Surface Waters. *Environ. Toxicol. Chem.* **2022**, *41* (10), 2375–2385. https://doi.org/10.1002/etc.5431.
(7) Weather Spark. Climate and Average Weather Year Round In Westerly. https://weatherspark.com/y/26174/Average-Weather-in-Westerly-Rhode-Island-United-States-Year-Round#Sections-Precipitation (accessed 2022-06-12).